*Proc. Indian natn Sci Acad.(PINSA)* **B68No.2** pp 217-234 (2002)

# Mechanisms of Iron-uptake and Iron-release in Lactoferrins

JAVED A KHAN, PRAVINDRA KUMAR, SUJATA SHARMA, ASHOK K MOHANTY, TALAT JABEEN, M PARAMASIVAM, SAVITA YADAV, A SRINIVASAN and TEJ P SINGH*
*Department of Biophysics, All India Institute of Medical Sciences, New Delhi 110029*

(Received on 23 July 2001; Accepted on 21 September 2001)

The current $Fe^{3+}$-containing tetrahedral intermediate of camel lactoferrin on the iron-binding pathway in domain-opened form and another tetrahedral intermediate of goat lactoferrin on the iron-release pathway in domain-closed conformation are the first demonstrations of intermediate states in the family of transferrin proteins. Lactoferrin binds $Fe^{3+}$ very tightly in a closed inter-domain cleft through coordination with four protein ligands (Asp 60/395, Tyr 92/433, Tyr 192/526 and His 253/595) and a synergistic anion, physiologically relevant, bidentate $CO_3^{2-}$. Upon $Fe^{3+}$-uptake, lactoferrins undergo a large scale conformational transition: the apo structure with an opening of the inter-domain cleft which is transformed into the closed holo structure, implying initial $Fe^{3+}$-binding in the open form. Similarly, upon $Fe^{3+}$-release, lactoferrins undergo large scale reverse conformational transition: the holo structure with the closed inter-domain cleft which is transformed into the open domain apo structure, implying initial release of $Fe^{3+}$ in the closed form. In order to understand the mechanism of iron-binding and -release, the structure of the two intermediates: one in the iron-binding pathway and the other in the iron-release pathway were determined. On the iron-binding pathway, a tetrahedral intermediate in which $Fe^{3+}$ was coordinated to two tyrosine and a bidentate $CO_3^{2-}$ in the domain-opened conformation. Similarly, on the iron-release pathway, the structure of a tetrahedral domain-closed intermediate through four protein ligands in which $CO_3^{2-}$ has already dissociated from the protein, has been determined. The two iron-containing intermediate on the iron-binding and iron-release pathways when compared with the holo form show strong local structural differences in the iron binding clefts. However, the structures of the rest of the proteins of the two intermediates on iron-binding and iron-released pathways are essentially similar to apo and holo forms respectively.

**Key Words: Camel lactoferrin, Intermediate, Apolactoferrin, X-ray diffraction, Goat lactoferrin**

## Introduction

Lactoferrins are iron-binding proteins. They serve to control the iron levels in the body fluids of vertebrates by their ability to bind very tightly two $Fe^{3+}$ ions (Aisen & Listowski 1980). They are ~ 80 kDa single-chain proteins and consist of two similar sized homologous N- and C- lobes, which are further divided into two similar sized domains (domains N1 and N2 in the N-lobe and domains C1 and C2 in the C-lobe). The iron-binding sites are located within the inter-domain cleft of each lobe. Crystal structures of diferric forms of human (HLF), bovine (CLF) equine (ELF) and buffalo (BLF) lactoferrins reveal that the two domains are closed over an $Fe^{3+}$ ion. Four of the six $Fe^{3+}$ coordination sites are occupied by the protein ligands of two tyrosine residues, one aspartic acid residue and one histidine residue, Asp 60(395), Tyr 92(433), Tyr 192 (526) and His 253(595) and the other two by a synergistically and physiologically relevant anion $CO_3^{2-}$ (Anderson et al. 1989, Moore et al. 1997, Sharma et al. 1998, Karthikeyan et al. 1999a, 2000).

*Corresponding author: *Tel.*: 0091-11-659-3201; *Fax* : 0091-11-686-2663; *E-mail*: tps@aiims.aiims.ac.in

For the iron-free apo form, however, X-ray crystallographic studies on human (HALF) (Jameson et al. 1998) equine (EALF) (Sharma et al. 1999, Kumar et al. 2001a), and camel (UALF) (Khan et al. 2001a) apolactoferrins and solution scattering analysis (Grossmann et al. 1998) have shown that the lactoferrins assume a conformation with an opening of the interdomain cleft. This implies that lactoferrin initially binds the $Fe^{3+}$ ion in the open form before being transformed into the closed holo form. Differential domain and hinge locations of the four protein ligands Asp 60(395) in the domain 1, Tyr 192(526) in the domain 2 and Tyr 92(433) and His 253(595) in different hinges inevitably require an alternative $Fe^{3+}$ coordination structure for the $Fe^{3+}$-loaded, domain-opened intermediate. Such an alternative structural state has been a central question to be solved for the understanding of the $Fe^{3+}$-binding pathway in lactoferrins.

On the other hand, on the pathway of iron-release from the holo-form, the initial step is protonation of the carbonate anion, resulting in the formation of bicarbonate. The reduction in charge on the anion results in movement of the bicarbonate anion away from the iron site in such a way that it becomes detached from the surroundings. This suggests the existence of an intermediate in closed conformation with four-fold iron coordination but without carbonate anion.

A major difficulty encountered in the structure analyses of these intermediates is to prepare stable protein forms. We were able to solve this problem by preparing these intermediates in solutions and then trapping them through simultaneous process of crystallization. We report here the results of structural investigations on various iron-saturated and iron-free lactoferrins, lactoferrin intermediates in the $Fe^{3+}$-binding and $Fe^{3+}$-release pathways. The observations strongly suggest that the two tyrosine residues are the initial $Fe^{3+}$-binding ligands in the open lactoferrin and the carbonate anion is the first to dissociate in the closed lactoferrin.

**Sequence Determination and Analyses**

So far, eight complete sequences of lactoferrins from different species have been determined either directly at the protein level or by translation from nucleotide sequences. These are from HLF (Metz-boutigue et al. 1984), ELF (Sharma et al. 1998) CLF (Pierce et al. 1991), BLF (Karthikeyan et al. 2000), GLF (Lydon et al. 1992), ULF (Kappeler et al. 1999, Khan et al. 2001a), MLF (Shirsat et al. 1992) and PLF (Provost et al. 1994). The chain lengths of lactoferrins from various sources are different (table 1). The multiple sequence alignment was carried out with CLUSTALW program (Thomson et al. 1994). These eight sequences have been aligned with the sequence of ELF (table 2). It reveals that the C-lobes of lactoferrins are highly conserved. The percentage sequence identity between various lactoferrins is given in table 3. It shows that lactoferrins from species within the same family e.g. CLF, BLF and GLF display a higher sequence identity which is of the order of 92%. The sequences of lactoferrin from species of different phylogenic families show lower sequence identities (<70%). Similarly, the sequence identities between the two molecular halves are also significantly high (35-40%) (table 4). As a result, the two lobes fold in a similar way. Further examination of sequences reveals that the amino acids involved in the binding of cation ($Fe^{3+}$) and anion ($CO_3^{2-}$) are conserved. There are in general, 17 disulphide bridges except human and murine lactoferrins where only sixteen disulphide bridges were observed. In porcine lactoferrin whose chain length is shorter by 20 amino acids on

**Table 1** *Number of amino acid residues in lactoferrin from different species*

| Species | Number of amino acids |
|---|---|
| Equine (ELF) | 689 |
| Goat (GLF) | 689 |
| Buffalo (BLF) | 689 |
| Bovine (CLF) | 689 |
| Camel (ULF) | 689 |
| Human (HLF) | 691 |
| Mouse (MLF) | 705 |
| Porcine (PLF) | 686 |

**Table 2** *The comparison of amino acid sequences of equine lactoferrin with other lactoferrins showing conserved regions (grey), metal binding sites (red), predicted glycosylation sites (pink), cysteine residues (yellow) with the residues involved in bacteriacidal acitvity (dark blue) and the highly conserved fragment of 10 residues (green) involved in antifungal role*

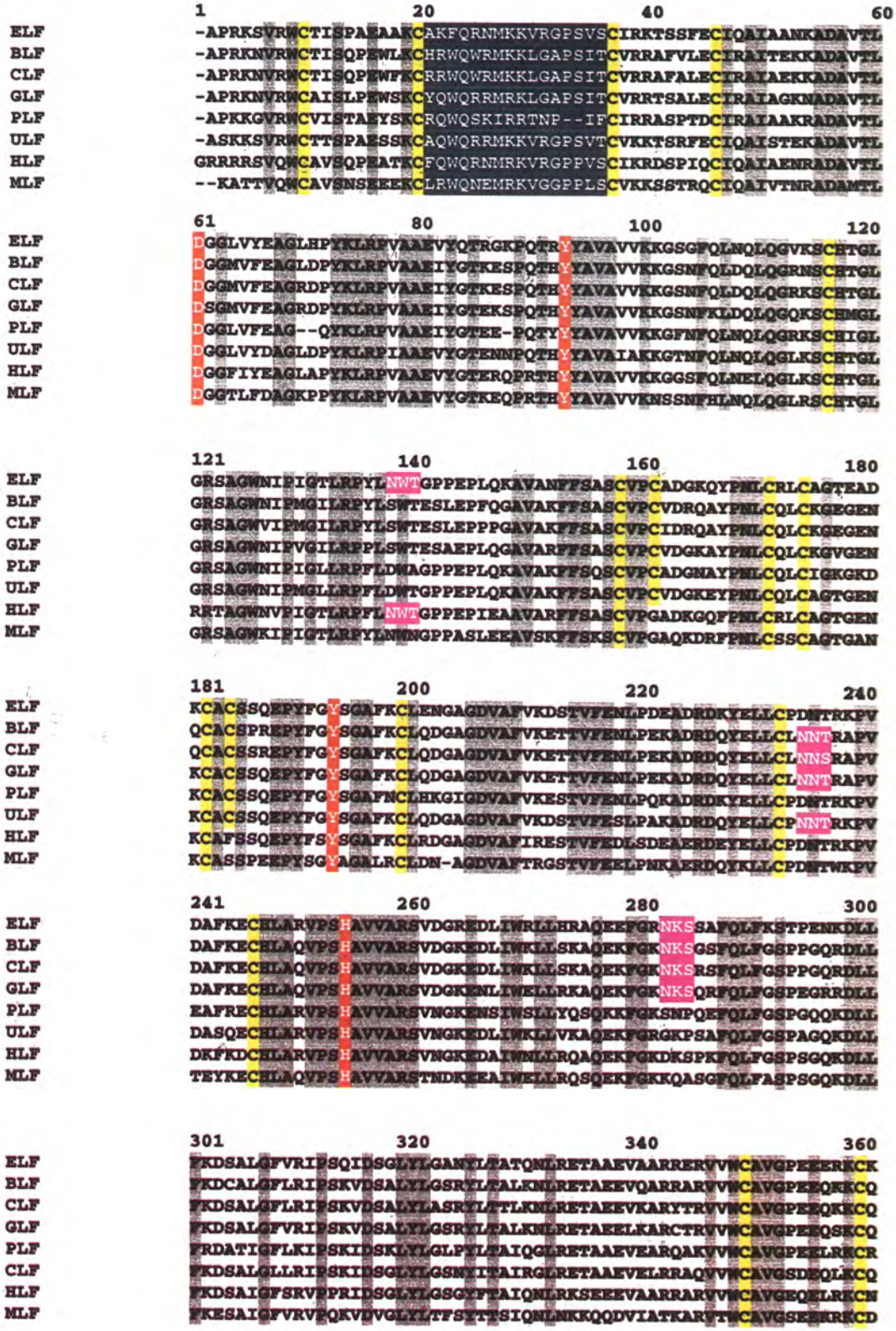

**Table 2** *(contd.)*

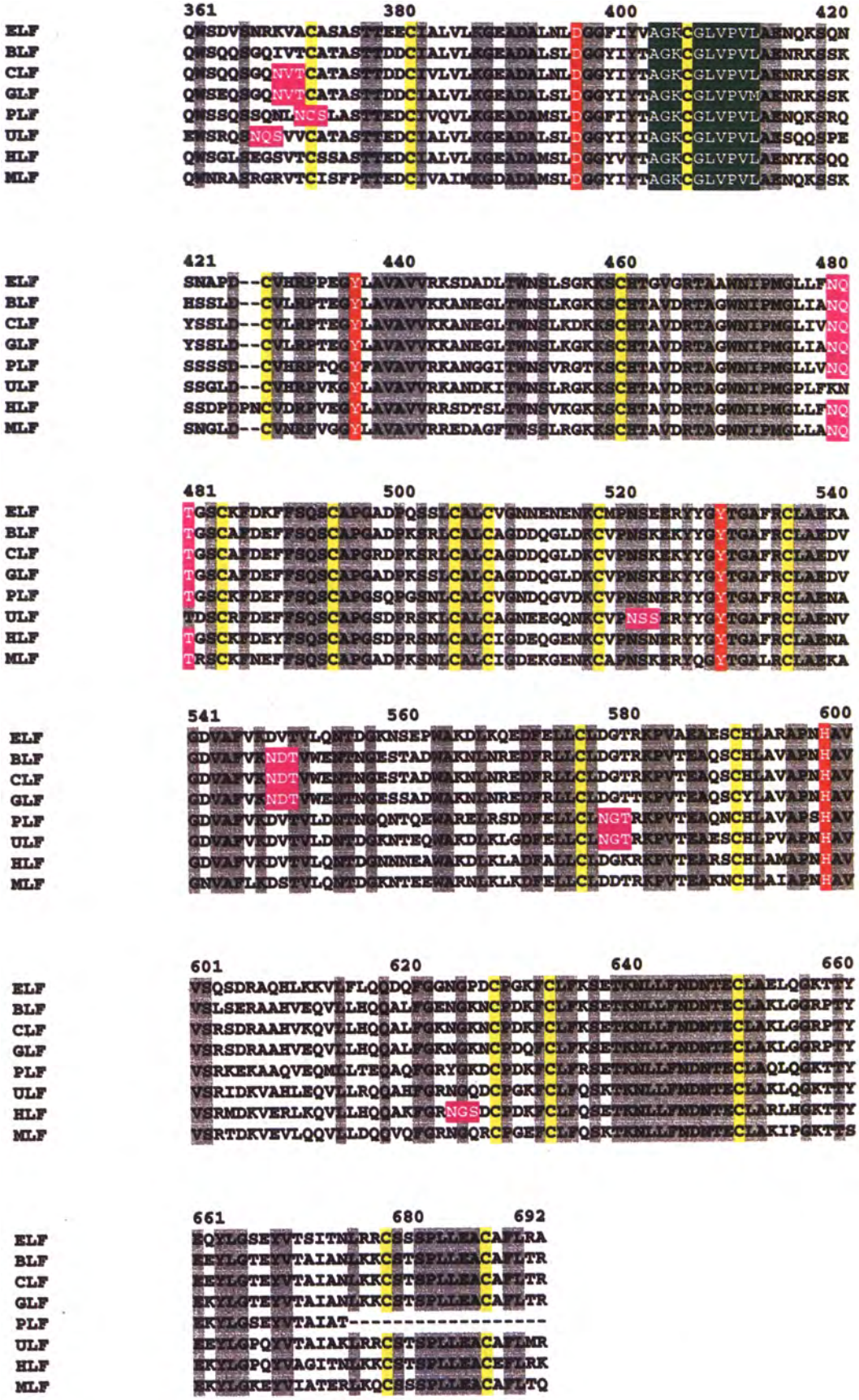

**Table 3** *Sequence identity between lactoferrins from different sources*

| | ELF | GLF | BLF | HLF | CLF | MLF | PLF | ULF |
|---|---|---|---|---|---|---|---|---|
| ELF | 100 | 72.4 | 72.8 | 75.0 | 72.4 | 65.6 | 68.9 | 77.2 |
| GLF | 72.4 | 100 | 91.4 | 70.2 | 91.7 | 63.9 | 72.5 | 74.6 |
| BLF | 72.8 | 91.7 | 100 | 69.9 | 95.9 | 64.0 | 70.5 | 75.8 |
| HLF | 75.0 | 70.2 | 64.4 | 100 | 69.4 | 70.4 | 70.4 | 74.2 |
| CLF | 72.4 | 91.7 | 95.9 | 69.4 | 100 | 70.0 | 70.4 | 74.6 |
| MLF | 65.6 | 63.9 | 64.0 | 64.0 | 64.0 | 100 | 60.8 | 66.8 |
| PLF | 68.9 | 72.7 | 70.5 | 70.4 | 70.4 | 60.8 | 100 | 71.8 |
| ULF | 77.2 | 74.6 | 75.8 | 74.6 | 74.6 | 71.8 | 71.8 | 100 |

**Table 4** *Interlobe sequence identity of lactoferrins*

| Species | Identity between N- and C- lobes identity (%) |
|---|---|
| **ELF** | **39** |
| **GLF** | **35** |
| *BLF* | *36* |
| *CLF* | *36* |
| **ULF** | **36** |
| *HLF* | *38* |
| **MLF** | **37** |
| **PLF** | **39** |

the C-terminus does not have the last two cysteines.

Furthermore, the number and locations of glycosylation sites also differ in various lactoferrins. The locations of glycosylation sites affect the binding to the receptors in certain cases. However, they dont influence the foldings of these proteins until located at the iron binding clefts. The reason as to why different numbers of glycosylation sites exist in various lactoferrins is not yet clear.

### Overall Molecular Structure

The polypeptide chains of lactoferrin folds into N- and C-lobes representing the N-terminal and C-terminal halves of the molecule each of which is folded into two domains (N1 and N2 ; C1 and C2 respectively Karthikeyan et al. 1999b). The structure of iron saturated (holo-form) lactoferrin revealed that the two domains of each lobe are closed over an $Fe^{3+}$ ion (figure 1). The structure of iron-free (apo-form) shows that its both lobes adopt open conformations (figure 2). In this case N2 and C2 domains move away from the N1 and C1 domains respectively as rigid bodies.

### Intermediates on the Iron-binding Sites

The transition from the open to closed conformation is expected to pass through an intermediate in which the $Fe^{3+}$ ion might be initially binding to the protein in the open form before being transformed into the closed holo-form. The four protein ligands have different locations (figure 3), and the iron-loaded open form is a possible transient intermediate towards the fully saturated holo-form with closed domains. The postulated reaction scheme of iron-binding is presented in figure 4. The study of intermediate III (figure 4) is necessary for revealing the pathway of $Fe^{3+}$-uptake in lactoferrins for understanding the folding of lactoferrins.

### Crystallization of intermediate LF-2$Fe^{3+}$-2$CO_3^{2-}$ (ULFI)

The crystals of the intermediate (figure 5) were obtained by a modified technique of microdialysis at 4°C (Khan et al. 2001b). The apo-form of dissolved protein in the buffer was loaded in the glass capillaries and placed in the vials containing the same buffer with 26% (v/v) ethanol. To this reservoir solution the excess amounts of $FeCl_3$ and $CO_3^{2-}$ were added. These setups allowed the diffusion of $Fe^{3+}$ and $CO_3^{2-}$ ions as well as the precipitating agent ethanol to the protein solution simultaneously. The crystals with pale yellow

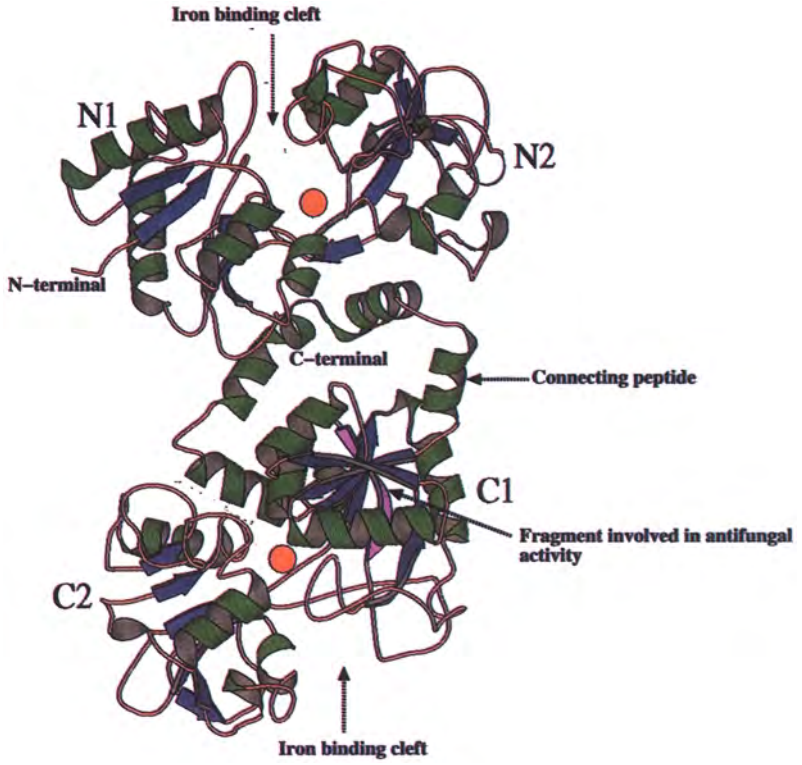


**Figure 1** Three-dimensional folding of buffalo lactoferrin showing N1, N2 and C1, C2 domains, iron-binding clefts, connecting helical peptide and a fragment involved in antifungal function (red). The figure was drawn with MOLSCRIPT (Kraulis 1991)

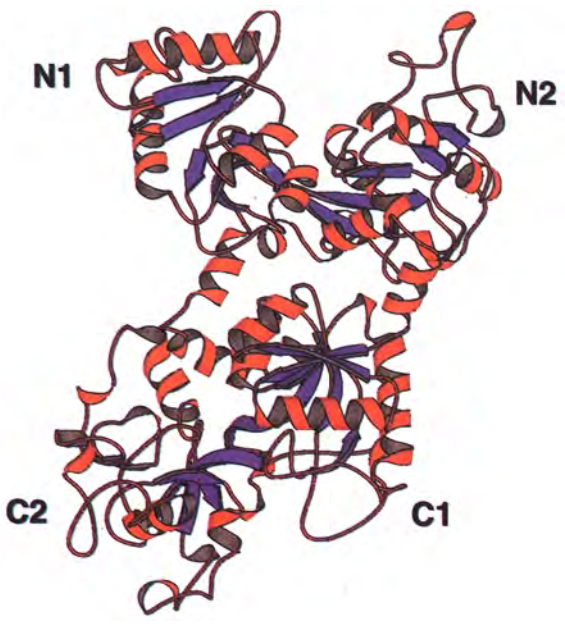


**Figure 2** Three-dimensional structure of camel apolactoferrin in which both lobes are widely opened. The figure was drawn with MOLSCRIPT (Kraulis 1991)

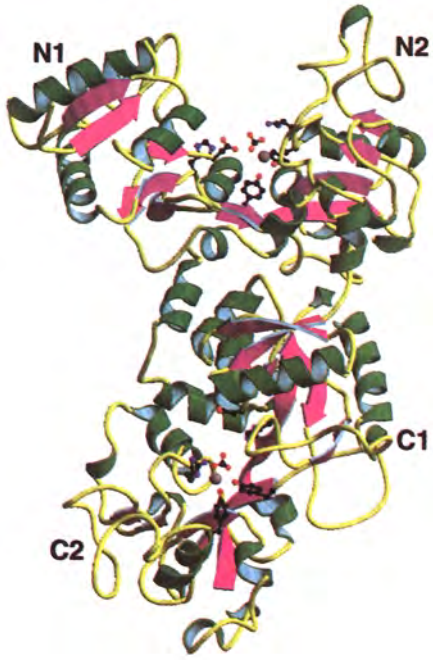


**Figure 3** Schematic representation of iron-saturated camel lactoferrin intermediate (ULFI). The figure was drawn using MOLSCRIPT (Kraulis 1991) and RASTER3D (Merritt & Murphy 1994)

$$\text{Apo-Lf} + 2CO_3^{2-} \longrightarrow \text{Lf-}2CO_3^{2-}$$
(Open) I → (Open) II

$$\text{Lf-}2CO_3^{2-} + 2FeCl_3 \longrightarrow \text{Lf-}2Fe^{3+}\text{-}2CO_3^{2-}$$
(Open) II → (Open tetrahedral) III

$$\text{Lf-}2Fe^{3+} - 2CO_3^{2-} \longrightarrow \text{Lf-}2Fe^{3+}\text{-}2CO_3^{2-}$$
(Open tetrahedral) III → (Closed octahedral) IV

**Figure 4** The postulated reaction scheme for iron-uptake in camel lactoferrin

**Figure 5** Crystals of camel lactoferrin tetrahedral intermediate on the iron-binding pathway

colour grew in two days. The iron content of the crystals was estimated from the ratio of $A_{465}$ / $A_{280}$ ( Mazurier et al. 1980). The iron saturation in the crystal was found to be of the order of 80%. These crystals were used for the intensity data collection and the structure was determined by molecular replacement method using the model of camel apolactoferrin (Khan et al. 2001a). The structure was refined to an R value of 0.187. In this structure, the iron atoms exist in the opened-up interdomain clefts. The two $Fe^{3+}$ ligating tyrosine residues in the holo-form Tyr 92(433) and Tyr 192(526) appear to participate in the iron coordination wheras the other two protein ligands of Asp 60(395) and His 253(595) are located far away from the iron atoms. The bidentate carbonate ions provide two oxygen atoms in each lobe to complete the tetrahedral coordinations of $Fe^{3+}$ ions. Overall, the structure of the lactoferrin intermediate is almost indistnguishable from that of apolactoferrin.

**The Structure of the $Fe^{3+}$ Binding Sites**

The iron coordination and hydrogen bonding structure of $CO_3^{2-}$ in the ULFI are illustrated in (figure 6 a-d). As summarized in table 5 the distances from the iron of Tyr 92-OH and Tyr 192-OH in N-lobe and of Tyr 433-OH and Tyr 526-OH in C-lobe of 2.7 Å, 2.7 Å and 2.8 Å, 2.4 Å respectively clearly show the involvement of tyrosine residues in the coordinations with $Fe^{3+}$ The other two protein ligands of Asp 60(395) and His 253(595) are not involved in the coordination with iron atom : the distances of Asp Od1 and His Ne2 from iron in the N- and C- lobes are 10.5 Å, 8.6 Å and 10.1 Å, 8.2 Å respectively. The other two coordinations of the tetrahedrally coordinated iron atom are provided by $CO_3^{2-}$ anion. The distances of $CO_3^{2-}$-O1 and $CO_3^{2-}$-O2 from iron in the N- and C-lobes are 2.8 Å, 2.8 Å and 2.6 Å, 2.6 Å respectively. The coordination distances in the present structure are slightly larger than those generally observed in the structures of lactoferrins

**Table 5** *Distances in metal and anion-binding sites*

| | | N-LOBE | C-LOBE |
|---|---|---|---|
| **A.** | **Coordinating metal-ligand distances (Å)** | | |
| | Fe - OH Tyr 92(433) | 2.7 | 2.8 |
| | Fe - OH Tyr 192(526) | 2.7 | 2.4 |
| | Fe - O1 (carbonate) | 2.8 | 2.6 |
| | Fe - O2 (carbonate) | 2.8 | 2.6 |
| **B.** | **Hydrogen bond lengths involving anions (Å)** | | |
| | O1 ... Og1 Ser 122(Thr 464) | 3.2 | 3.2 |
| | O1 ... OW | 3.0 | 3.2 |
| | O2 ... NE Arg 121(463) | 3.2 | 3.0 |
| | O3 ... NH2 Arg 121(463) | 3.0 | 2.7 |

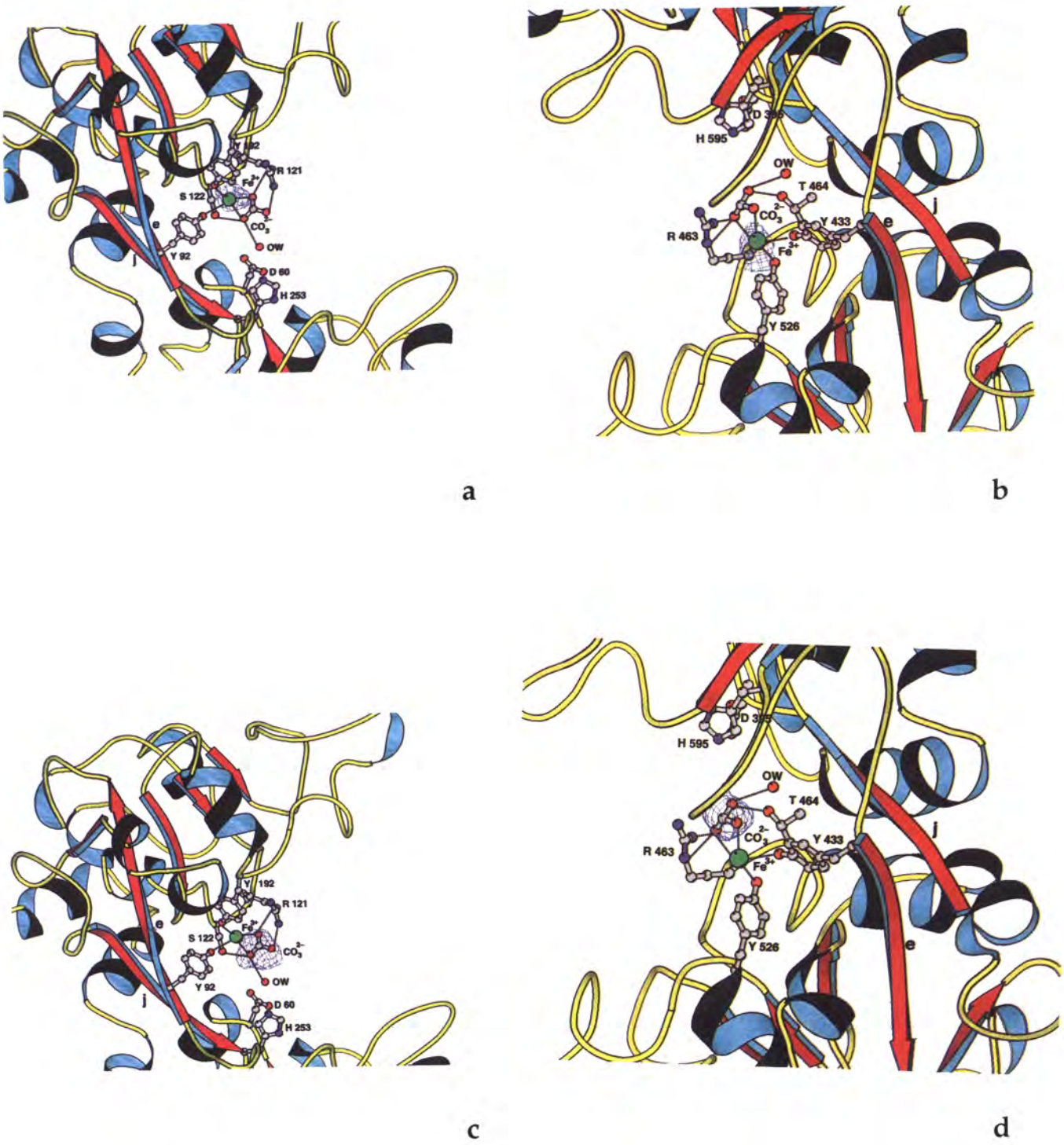


**Figure 6 (a-d)** The (Fo-Fc) omit map for (a) N-lobe, (b) C-lobe showing the electron density for $Fe^{3+}$ ion at 4 s level and the Fo-Fc omit map for (c) N-lobe and (d) C-lobe showing the electron density for $CO_3^{2-}$ ion at 2.5 s level. The dotted lines indicate metal ion coordinations and hydrogen bonded interactions involving anion. The figure was drawn using BOBSCRIPT (Esnouf 1997)

(Anderson et al. 1989, Moore et al. 1997, Sharma et al. 1998, Karthikeyan et al. 1999a, 2000) suggesting the formation of slightly loose coordinations.

The carbonate ion is stabilized by hydrogen bonded interactions with Arg 121(463) involving Ne and NH2 at distances of 3.2 Å and 3.0 Å in N-lobe and 3.0 Å and 2.7 Å in C-lobe. The other interactions of anion which are different in ULFI involve a hydrogen bond with Ser 122Og in N-lobe and Thr 464Og in C-lobe. In addition to it a water molecule is present in each lobe to form a hydrogen bond with $CO_3^{2-}$. In the present structure, anion lacks two hydrogen bonds with backbone nitrogen atoms of residues 123(465) and 124(466) which are present in the iron saturated forms of other lactoferrins. The residues 121-124(463 - 466) are part of the positively charged anion binding pocket. Though it has gained a hydrogen bond through a water molecule in each but overall the anions remain slightly loosely bound in the structure of intermediate.

**Intermediate on the Iron-release Pathway**

Similarly, the transition from the closed to open conformation is expected to pass through an intermediate in which anion is lost while ferric ion is still bound to the protein in closed conformation before being transformed into the open apo-form. The postulated reaction scheme of iron-release is presented in figure 7. The study of intermediate III (figure 7) is necessary for revealing the pathway of iron-release in lactoferrins for the understanding of unfolding of lactoferrins. The

| | | |
|---|---|---|
| Lf-2Fe$^{3+}$-2CO$_3^{2-}$ | ⟶ | Lf-2Fe$^{3+}$ + 2CO$_3^{2-}$ |
| (Closed octahedral) | | (Closed octahedral) |
| I | | II |
| Lf-22Fe$^{3+}$ | ⟶ | Lf-2Fe$^{3+}$ |
| (Closed tetrahedral) | | (Closed tetrahedral) |
| II | | III |
| Lf-2Fe$^{3+}$ | ⟶ | Apo-Lf + 2Fe$^{3+}$ |
| (Closed tetrahedral) | | (Open) |
| III | | IV |

**Figure 7** Reaction scheme of iron-releasing pathway in lactoferrins. Intermediate III has been crystallized

crystals of the intermediate III of goat lactoferrin were obtained by microdialysis method with protein concentration of 60 mg/ml in 0.025 M Tris-HCl at *p*H 7.0 (Kumar et al. 2001c). At *p*H 7.0 goat lactoferrin is present as a crystallographically stable intermediate that results from the protonation of the carbonate anion. In this model for iron-release from lactoferrin, the initial step is protonation of the carbonate anion, resulting in the formation of bicarbonate. The reduction in charge on the anion results in movement of the carbonate anion away from the iron site in such a way that it becomes detached from the helix 5 N terminus (figure 8). As a result of this the side chain of Arg 121 moves to a position where the carbonate anion is stabilized in the iron-bound state. The net result of this conformational change is the complete removal of anion from the iron-binding cleft.

**Crystallization of intermediate Lf-2Fe$^{3+}$ (GLFI)**

The crystals of the intermediate (figure 9) were obtained at *p*H 7.0 as in goat lactoferrin $CO_3^{2-}$ has been found to be dissociated from the protein at *p*H 7.0 but $Fe^{3+}$ was still present. 60 mg of protein was dissolved in 0.025 M Tris-HCl at *p*H 7.0. The solution was dialyzed against the same buffer containing 21% (v/v) ethanol at *p*H 7.0. The structure was determined by molecular replacement method using the model of iron-saturated buffalo lactoferrin (Karthikeyan et al. 1999a). The structure was refined to an R-factor of 0.246. The structure of goat lactoferrin intermediate (GLFI) reveals that the molecule is folded into two globular lobes, the N-lobe comprising the N-terminal half of the polypeptide chain (residues

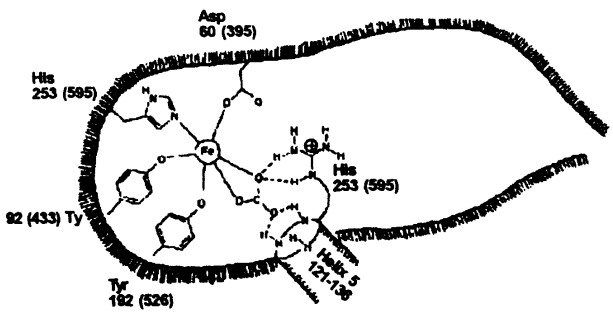


**Figure 8** Schematic diagram of iron site in each lobe of lactoferrin molecule

1-333), C-lobe comprising C-terminal half of the polypeptide chain (residues 345-689) and a connecting helical peptide (residues 334-344). Each lobe is further subdivided into two domains of approximately 160 residues each (figure 10)

The structure of GLFI is the first example where $CO_3^{2-}$ is absent. The iron coordination in GLFI is illustrated in figure 11 a-b. As summarized in table 6, the distances of iron with four protein ligands in both N- and C-lobes are optimum. The other two coordination with $CO_3^{2-}$ are absent.

## Discussion

X-ray crystallographic (Anderson et al. 1989, Moore et al. 1997, Sharma et al. 1998, Karthikeyan et al. 1999a, 2000) and solution scattering (Grossman et al. 1992, 1993, 1998) studies have revealed, that upon $Fe^{3+}$ uptake, lactoferrins undergo a large scale conformational transition from the domain-opened apo structure into the closed holo structure. Similarly upon iron-release lactoferrins undergo a conformational change from the closed iron-saturated structure to the domain-opened apo structure. The structural pathways for these reversible large-scale conformational transitions are not yet understood. The structures of iron-saturated carbonate containing domain-opened camel lactoferrins intermediate (ULFI) and iron-saturated carbonate deficient domain-closed goat lactoferrin intermediate (GLFI) will provide crucial information about the structural mechanism for the $Fe^{3+}$-binding and release. The crystal structure of ULFI demonstrates essentially the same open conformation as camel apolactoferrin (UALF) (figure 12) whereas the structure of GLFI is found similar to that of the closed iron-saturated holo form (figure 13). The structure of ULFI is clearly consistent with an iron-uptake mechanism shown schematically in figure 14. The positive macro-dipole at the N-terminal of helix 5 with Arg 121 in the vicinity are oriented towards the metal binding site making unfavorable environment to receive a ferric cation. This configuration readily explains the requirement for the synergistic carbonate anion which effectively neutralizes the positive charges and confers the site specificity for the binding of ferric ions. Therefore, the critical steps in the mechanism of iron-binding involve an early entry

**Table 6** *Distances in metal-binding sites*

| | | N-LOBE | C-LOBE |
|---|---|---|---|
| **A.** | **Metal-ligand bond lengths ( A)** | | |
| | Fe - $O^{\delta 1}$ Asp60 (395) | 2.08 | 1.85 |
| | Fe - OH Tyr92 (433) | 1.76 | 1.95 |
| | Fe - OH Tyr192 (526) | 2.24 | 2.05 |
| | Fe - $N^{\varepsilon 2}$ His253 (433) | 2.10 | 2.38 |

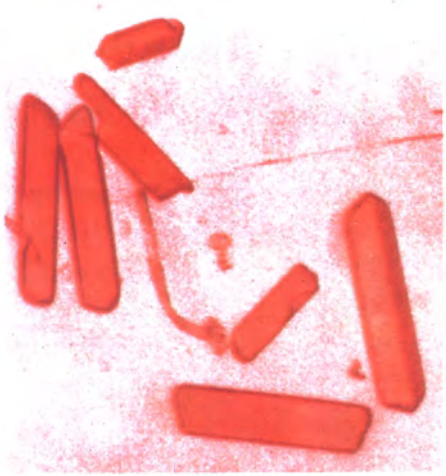

**Figure 9** Crystals of goat lactoferrin tetrahedral intermediate on the iron-releasing pathway

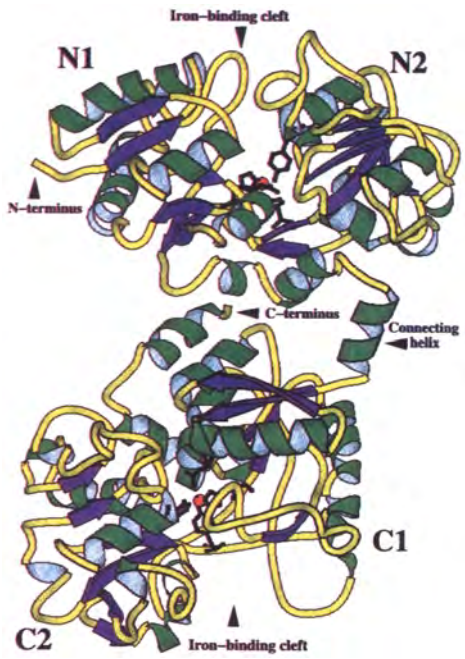


**Figure 10** Schematic representation of goat lactoferrin molecule showing the folding of domains and the location of ferric ion (red)

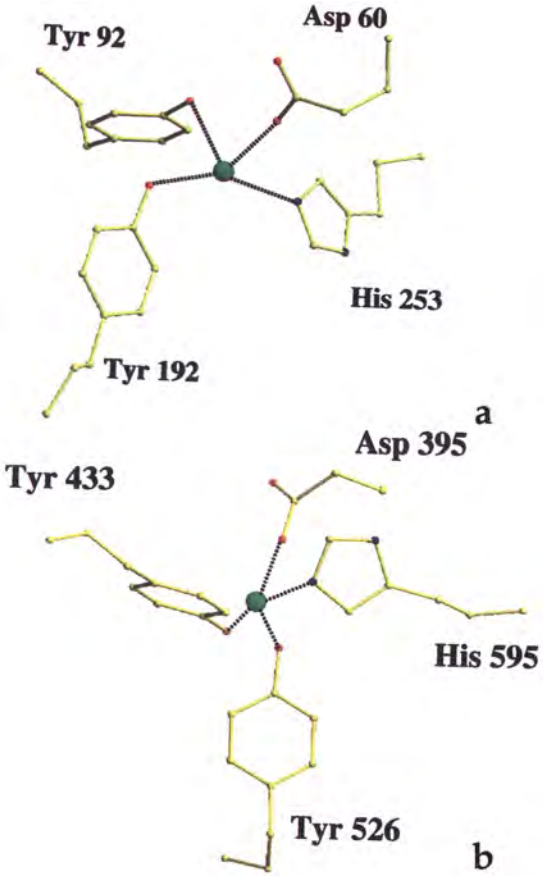


**Figure 11** The tetrahedral coordination for $Fe^{3+}$ ion in (a) N-lobe (b) C-lobe of goat lactoferrin

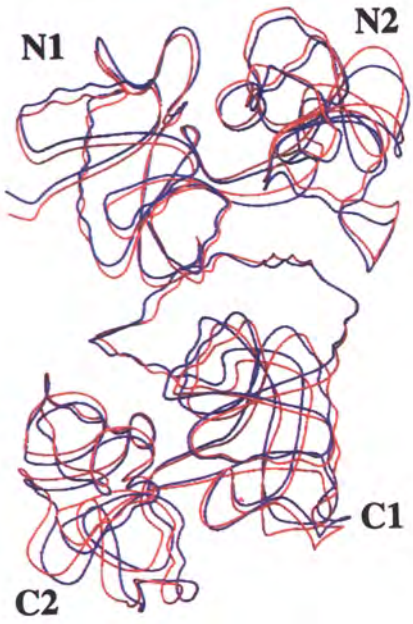


**Figure 13** Overall backbone superposition of GLFI (red) and BLF (cyan)

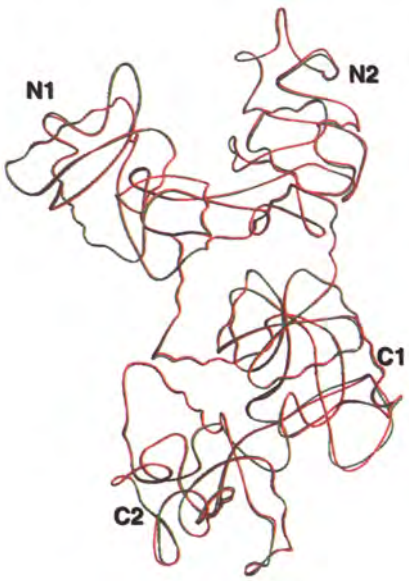


**Figure 12** Superimposition of the Ca traces of ULFI (red) and UALF (green). The r.m.s shifts of the Ca atoms and of the main chain atoms are 0.5 Å and 0.6 Å respectively. The figure was drawn using MOLSCRIPT (Kraulis 1991) and RASTER3D (Merritt & Murphy 1994)

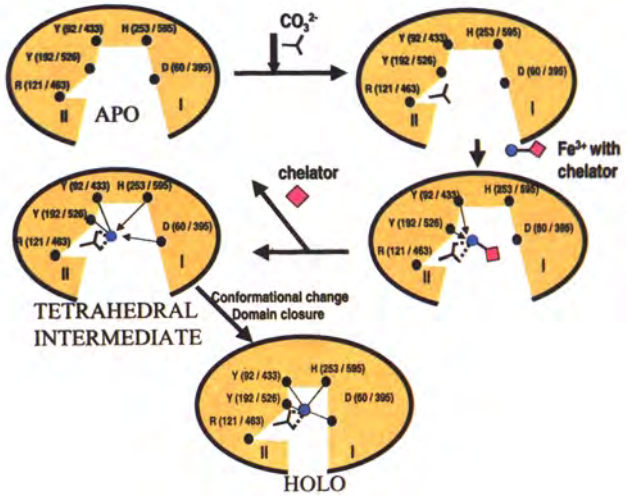


**Figure 14** A schematic representation of the mechanism of iron-uptake in lactoferrin molecule. The two tyrosine residues involved in iron-binding are Tyr 92(433) and Tyr 192(526)

of $CO_3^{2-}$ ions to interact with Arg 121(463) in the positively charged anion binding site of domain 2. The binding of carbonate anion induces a conformational change in the side-chain of Arg 121(463). This is the first conformational change in the protein in the mechanism of iron binding. This corresponds to intermediate III (figure 14) but is extremely short-lived as the iron-binding follows it almost instantaneously. These events occur in the proximity of two tyrosine residues 92(433) and 192(526) thus preparing it for iron-binding. As a result of it, the iron binds to the combination of two tyrosine residues and a carbonate ion first to form a tetrahedral intermediate. This appears to be a relatively stable intermediate. It is noteworthy that upon binding to $Fe^{3+}$, Tyr 92(433) and Tyr 192(526) shift in the present structure from their original positions in camel apolactoferrin. The largest displacement between any two corresponding atoms in the N-lobe was 0.7 Å while it was 1.9 Å in the C-lobe (figure 15). Yet another striking difference between the structures of the present intermediate and those of the iron-saturated forms of lactoferrin pertains to the positioning of $Fe^{3+}$ and $CO_3^{2-}$ ions. While the positioning of $Fe^{3+}$ is only slightly different in ULFI, the $CO_3^{2-}$ occupies a substantially displaced position. Since, the lobes are

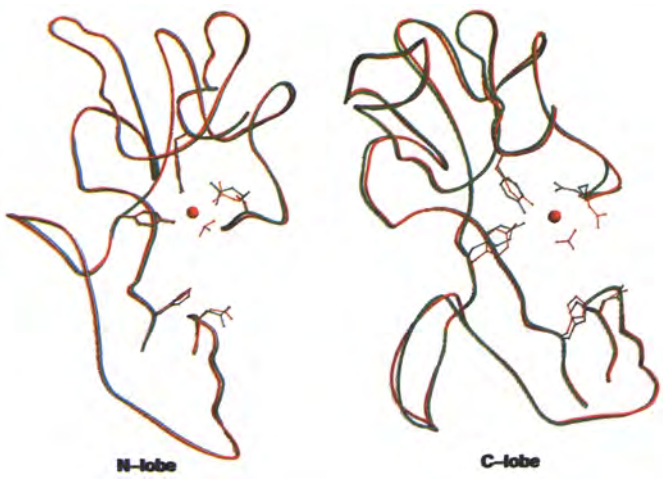


**Figure 15** Superposition of Ca traces of regions around iron-binding clefts and iron-binding residues of ULFI (red) and UALF (green). The r.m.s shifts of the residues in C-lobe are more pronounced than in N-lobe. The figure was drawn using MOLSCRIPT (Kraulis 1991) and RASTER3D (Merritt & Murphy 1994)

in open conformation, the $Fe^{3+}$ forms only four coordination links. These four bonds though weaker but are geometrically identical to those observed in the structures of iron-saturated lactoferrins (Anderson et al. 1989, Moore et al. 1997, Sharma et al. 1998, Karthikeyan et al. 1999a, 2000). On the other hand, the hydrogen bonded interactions of $CO_3^{2-}$ anion with the protein are substantially different. While the two key interactions with Arg 121(463) are similar, the other links are different. As seen from figures 16 (a-d) in HLF and BLF, the remaining three hydrogen bonds involve Thr 117(459) Og and backbone nitrogen atoms of Ala 123(465) and Gly 124(466). In contrast in the present structure, there are a total of only four hydrogen bonds. Two of them are with Arg 121(463) and out of remaining two, one is with Ser 122 Og in N-lobe and Thr 464 Og1 in C-lobe and one each with solvent water molecule. Overall, the hydrogen bonding pattern of $CO_3^{2-}$ in the intermediate is different from diferric lactoferrins. The $CO_3^{2-}$ anion is also less tightly held in the intermediate leaving a scope for an adjustment on final folding.

The crystal structure of GLFI (III in figure 17) suggests that this is a stable intermediate involved in the release of iron from lactoferrin. The information provided by the crystal structure is crucial to delineate the mechanism of iron-release. The structure of GLFI is clearly consistent with an iron-release mechanism shown schematically in figure 17. The crystals were grown at a *pH* where protonation of carbonate occurs. The protonation of the carbonate anion results in the movement of the bicarbonate anion away from the iron site in such a way that it becomes detached from the helix 5 N-terminus (figure 18). As a result of this, the hydrogen bonding involving anion is destabilized. It also causes displacement in the position of Arg 121(463). The net result of this conformational change is the removal of the anion from the metal binding site as a result of substantial weakening of the hydrogen bonding between the anion and the protein (figure 18 a-b). The carbonate protonation and the loss of hydrogen binding is followed by slow protonation of the protein ligands with subsequent release of the metal ion. On removal of the metal ion the cleft opening occurs.

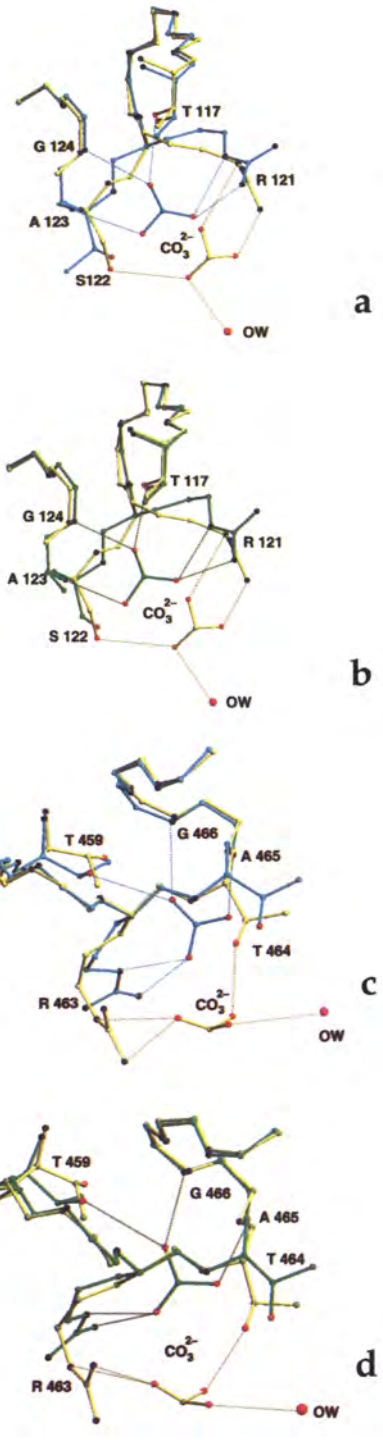


**Figure 16** Superpositions of anion binding pockets in the N-lobes of (a) HLF (cyan) and ULFI (yellow) and (b) BLF (green) and ULFI (yellow). Similarly Superpositions of anion binding pockets in the C-lobes of (c) HLF (cyan) and ULFI (yellow) and (d) BLF (green) and ULFI (yellow). The dotted lines indicate the hydrogen bonded interactions between protein and anion. The figure was drawn using MOLSCRIPT (Kraulis 1991) and RASTER3D (Merritt & Murphy 1994)

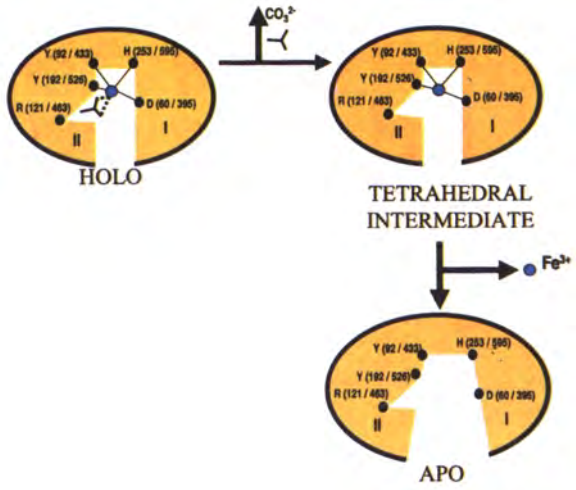


**Figure 17** A schematic representation of the mechanism of iron-release in lactoferrins

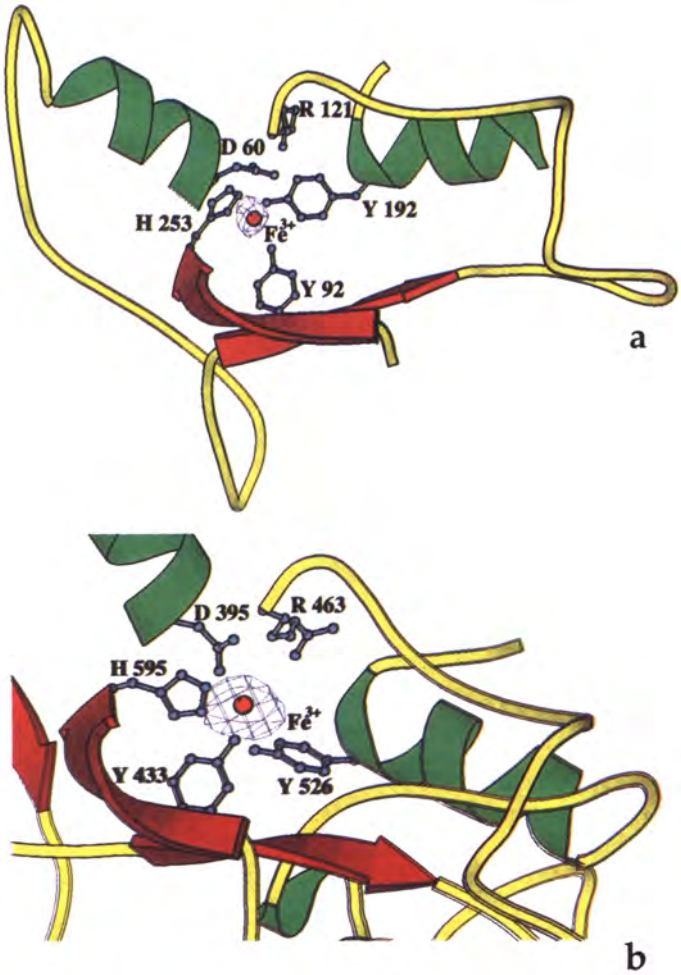


**Figure 18** The difference fourier (Fo-Fc) map showing the electron density for $Fe^{3+}$ in (a) N-lobe and (b) C-lobe. The contours are drawn at 3σ level

The crystal structures of human copper lactoferrin at 2.1 Å resolution (Smith et al. 1992) and equine summarium-lactoferrin (Sharma et al. 1999) have shown that the metal-binding sites in N- and C-lobes are different whereas the C-lobe site is a distorted octahedral with an asymmetrically bidentate anion, the N-lobe site is square pyramidal with monodentate. These changes are accommodated in the structure by small movements of the metal ion, anion and Arg 121 side-chain within each binding site without affecting the overall protein structure.

The position of iron in GLFI is similar to that observed in other diferric lactoferrins (Kumar et al. 2001c). However there is a slight change in the position of protein ligands. Similarly, the positions of protein ligands and metal ions in ULFI are also different from those observed in other diferric forms (Anderson et al. 1989, Moore et al. 1997, Sharma et al. 1998, Karthikeyan et al. 1999a, 2000 Khan et al. 2001). The superposition of protein ligands and $Fe^{3+}$ ion of ULFI and GLFI (figure 19 a-b) show significant displacements from each other suggesting that a process of rearrangements of various elements in the iron binding clefts occurs differently when following the paths of iron-uptake and iron-release. The overall structures of two intermediates are completely different because the intermediate on the iron-binding pathway is in the open-form while the one on the iron-release pathway is still in the closed conformation. However, the superimpositions of open-form ULFI with an apo-form and that of GLFI with a holo-form show good agreements suggesting that the changes taking place in the iron-binding clefts during the process of iron binding and iron release do not affect the rest of the protein structure.

In conclusion, the previous crystallographic structures of lactoferrins have been restricted essentially to the two structural forms, one in domain-opened iron-free apo-form (Rawas et al. 1997, Jameson et al. 1998, Kurokawa et al. 1999, Sharma et al. 1999, Khan et al. 2001a,) and the other, the domain-closed, $Fe^{3+}$-loaded holo-form (Anderson et al. 1989, Moore et al. 1997, Sharma et al. 1998, Karthikeyan et al. 1999a, 2000). The two alternative structural states, one on the iron-binding pathway and the other on the iron-release pathway have been observed for the first time and clearly demonstrates the $Fe^{3+}$-loaded open-form and $CO_3^{2-}$ deficient $Fe^{3+}$-loaded closed form. The one on the iron-binding pathway shows the binding of iron in the domain-opened form with tetrahedral coordination. In this model, only the two tyrosine residues 92(433) and 192(526)

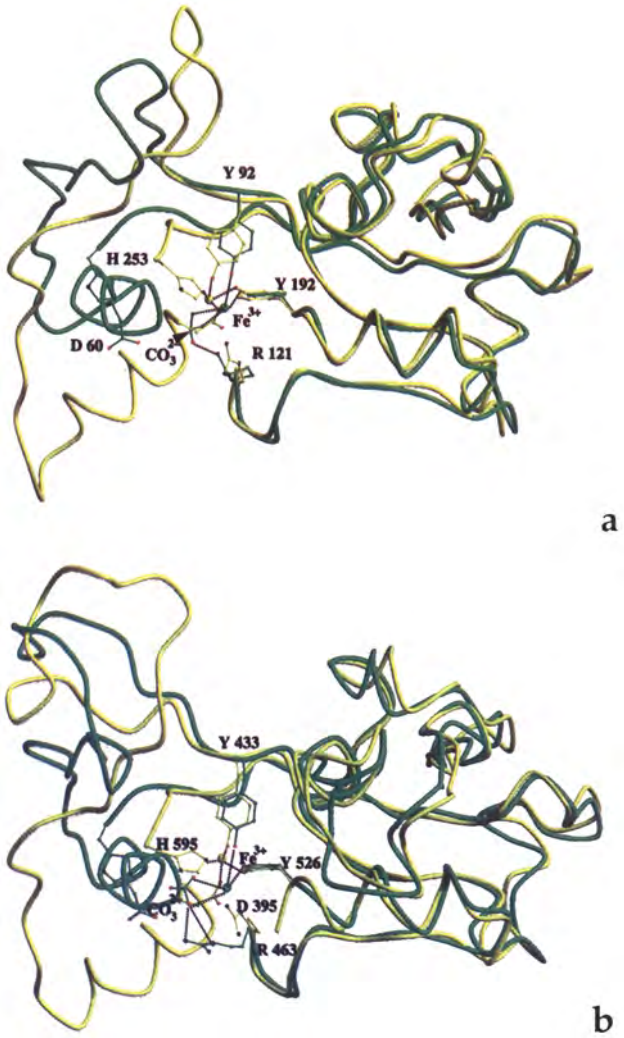


***Figure 19*** *The superimposition of Ca traces of camel* lactoferrin tetrahedral intermediate on the iron binding pathway in (a) N-lobe and (b) C-lobes. The side-chains of iron-binding ligands and the coordination to iron are also indicated.

participate in the $Fe^{3+}$ coordination as protein ligands (figure 6a-d, table 5). The coordination structure by the two tyrosine residues is consistent with the earlier hypothetical structure for the $Fe^{3+}$-loaded, domain-opened transferrin intermediate (Baker & Lindley 1992). Regardless of whether the Lf-$Fe^{3+}$-$CO_3^{2-}$ intermediate assumes the open or closed conformation in solutions, the finding that the overall structure of the interm ediate is almost indistinguishable from that of apo form (figure 12) is consistent with the view that the two tyrosine residues are the protein ligands for the $Fe^{3+}$ entry in the intact lactoferrin lobe with domain-opened conformation. The other one, on the iron-releasing pathway shows the binding of iron without $CO_3^{2-}$ in the domain-closed form with tetrahedral coordination. In this model, the two coordinations from the bidentate $CO_3^{2-}$have been lost. This is the first structural evidence of a domain-closed conformation without $CO_3^{2-}$ anion while the iron is still bound to the protein. It is an important finding that $CO_3^{2-}$ is lost first while the domains are still in the closed conformations.

The present two intermediates in the opposite pathways with different binding arrangements and in different structural environments of the iron binding clefts tend to attain similar stabilities before the final turnover. These studies have clearly established the mechanisms of iron-binding and iron-release in lactoferrins. Further studies on intermediates from other species at high resolutions will provide additional details for generalizing the mechanisms of iron-uptake and iron-release in the proteins of lactoferrin/ transferrin family.

**Acknowledgements**

The work was supported by a grant from the Department of Biotechnology, New Delhi. Javed A Khan, Pravindra Kumar and M Paramasivam thank the Council of Scientific Research, New Delhi for the award of Senior Research Fellowships.

## References

Aisen and Listowski 1980 Iron transport and storage proteins; *Annu. Rev. Biochem.* **49** 357-393

Anderson B F, Baker H M, Norris G E, Rice D E and Baker E N 1989 Structure of Human Lactoferrin: crystallographic structure analysis and refinement at 2.8 Å resolution; *J. Mol. Biol.* **209** 711-734

Baker E N and Lindley P F 1992 New perspectives on the structure and function of transferrins; *J. Inorg. Biochem.* **47** 147-160

Grossmann J G, Neu M, Pantos E, Schwab F J, Evans R W, Townes-Andrews E, Lindley P F, Appel H, Thies W G and Hasnain S S 1992 X-ray solution scattering reveals conformational changes upon iron uptake in lactoferrin, serum and ovo-transferrins; *J. Mol. Biol.* **225** 811-819

_____, Mason A B, Woodworth R C, Neu M, Lindley P F and Hasnain S S 1993 Asp ligand provides the trigger for closure of transferrin molecules. Direct evidence from X-ray scattering studies of site-specific mutants of the N-terminal half-molecule of human transferrin; *J. Mol. Biol.* **231** 554-558

Esnouf R M 1997 An extensively modified version of MolScript that includes greatly enhanced coloring capabilities; *J. Mol. Graphics* **15** 132-134

Grossmann J G, Crawley J B, Strange R W, Patel K J, Murphy L M, Neu M, Evans R W and Hasnain S S 1998 The nature of ligand-induced conformational change in ransferrin in solution. An investigation using X-ray scattering, XAFS and site-directed mutants; *J. Mol. Biol.* **279** 461-472

Jameson G B, Anderson B F, Norris G E, Thomas H D and Baker E N 1998 Structure of human apolactoferrin at 2.0 Å resolution. Refinement and analysis of ligand induced conformational change; *Acta Crystallogr. Sec D* **54** 1319-1335

Kappeler S, Farah Z and Puhan Z 1999 Alternative splicing of lactophorin mRNA from lactating mammary gland of the camel (*Camelus dromedarius*); *J. Dairy Sci.* **82** 2084-2093

Karthikeyan S, Yadav S, Paramasivam M, Srinivasan A and Singh T P 1999a Structure of buffalo lactoferrin at 2.5 Å resolution using crystals grown at 303K shows different orientations of the N and C lobes; *Acta Crystallogr. Sec. D***55** 1805-1813

Karthikeyan S, Sharma S, Sharma A K, Paramasivam M, Yadav S, Srinivasan A and Singh T P 1999b Structural variability and functional convergence in lactoferrins; *Curr. Sci.* **77** 241-255

_____, Yadav S, Paramasivam M, Srinivasan A and Singh T P 2000 Structure of buffalo lactoferrin at 3.3 Å resolution at 277 K; *Acta Crystallogr. Sec. D***56** 684-689

Khan J A, Kumar P, Paramasivam M, Yadav R S, Sahani M S, Sharma S, Srinivasan A and Singh T P 2001a Camel lactoferrin- a transferrin-cum-lactoferrin : Crystal structure of camel apolactoferrin at 2.6 Å resolution and structural basis of its dual role; *J. Mol. Biol.* **309** 751-761

_____, Kumar P, Srinivasan A and Singh T P 2001b Protein intermediate trapped by the simultaneous crystallization process: Crystal structure of an iron-saturated intermediate in the $Fe^{3+}$ binding pathway of camel lactoferrin at 2.7 Å resolution; *J. Biol. Chem.* (2761, 36817-36823)

Kraulis P J 1991 MOLSCRIPT: a program to produce both detailed and schematic plots of protein structures; *J. Appl. Crystallogr.* **24** 946-950

Kumar P, Yadav S and Singh T P 2001a Structure of mare apolactoferrin at 3.2 Å resolution using the crystals grown at 30°C; *Acta crystallogr. Sec.* D (In press)

_____, Yadav S and Singh T P 2001b A novel 40 kDa protein from goat mammary secretions: Purification, crystallization and preliminary X-ray diffraction studies; *Acta Crystallogr. Sec.* D (In press)

_____, Yadav S and Singh T P 2001c Crystallization and structure determination of goat lactoferrin at 4.0 Å resolution: A new form of packing in lactoferrins with a high solvent content jn crystals; *Ind. J. Biochem. Biophys.* (In press)

Kurokawa H, Dewan J, Mikami B, Sacchettini J C and Hirose M 1999 Crystal structure of hen apo-ovotransferrin; *J. Biol. Chem.* **273** 28445-28452

Lydon J P, Malley B R, Saucedo O, Lee T, Headon R R and Coneely O M 1992 Nucleotide and primary amino acid sequence of porcine lactoferrin; *Biochim. Biophys. Acta* **1132** 97-99

Mazurier J and Spik G 1980 Comparative study of the iron binding properties of human transferrins. I. Complete and sequential iron saturation and desaturation of the lactotransferrin; *Biochim. Biophys. Acta* **629** 399-408

Merritt E A and Murphy M E P 1994 Raster3D version 2.0. A program for photorealistic molecular graphics; *Acta Crystallogr.* **D50** 869-873

Metz-Boutique M, Jolles J, Mazurier J, Schoentger F, Legrand D, Spik G, Montreul J and Jolles P C 1984 Human lactotransferrin: amino acid sequence and structural comparisons with other transferrins; *Eur. J. Biochem.* **145** 659-676

Moore S A, Anderson B F, Groom C R, Haridas M and Baker E N 1997 Three-dimensional structure of diferric bovine lactoferrin at 2.8 Å resolution; *J. Mol. Biol.* **274** 222-236

Pierce A., Colavizza D, Benaissa M, Maes P, Tartar A, Montreuil J and Spik J 1991 Molecular cloning and sequence analysis of bovine lactotransferrins; *Eur. J. Biochem.* **196** 177-184

Provost F L, Nocart M, Guerin G and Martin P 1994 Characterization of the goat lactoferrin cDNA: Assignment of the relevant locus to bovine U12 Synteny Group; *Biochem. Biophys. Res. Commun.* **203** 1324-1332

Rawas A, Muirhead H and Williams J 1997 Structure of apo duck ovotransferrin: the structures of the N and C lobes are in the open form; *Acta crystallogr.* **D53** 464-468

Sharma A K, Paramasivam M, Srinivasan A, Yadav M P and Singh T P 1998 Three-imensional structure of mare diferric lactoferrin at 2.6Å resolution; *J. Mol. Biol.* **289** 303-317

_____, Rajashankar K R, Yadav M P and Singh T P 1999 Structure of mare apolactoferrin: the N and C lobes are in the closed form; *Acta Crystallogr.* **D55** 1052-1057

_____ and Singh T P 1999 Lactoferrin-metal interactions: first crystal structure of a complex of lactoferrin with a lanthanidei on (Sm3+) at 3.4 Å resolution; *Acta Crystallogr.* **D55** 1799-1804

Shirsat N V, Bittenbender S, Kreider B L and Rovera G 1992 Structure of the murine lactotransferrin gene is similar to the structure of other transferrin-encoding genes and shares a putative regulatory region with the murine myeloperoxidase gene; *Gene.* **110** 229-233

Smith C A, Anderson B F, Baker H M and Baker E N 1992 Metal substitution in transferrins: the crystal structure of copper-lactoferrin at 2.1 Å resolution; *Biochemistry* **31** 4527-4533

Thompson J D, Higgins D G and Gibson T J 1994 CLUSTAL W: improving the sensitivity of progressive multiple sequence alignment through sequence weighting, position-specific gap penalties and weight matrix choice; *Nucl. Sci. Res.* **22** 4673-4680.